Numerical investigation of the plasma-aided fabrication of stoichiometric InAs nanodots at early stage of the growth

M. Alizadeh, H. Mehdipour, B. T. Goh, and S. A. Rahman

Citation: Journal of Applied Physics **114**, 024301 (2013); doi: 10.1063/1.4813116
View online: http://dx.doi.org/10.1063/1.4813116
View Table of Contents: http://scitation.aip.org/content/aip/journal/jap/114/2?ver=pdfcov
Published by the AIP Publishing

Numerical investigation of the plasma-aided fabrication of stoichiometric InAs nanodots at early stage of the growth

M. Alizadeh,[1] H. Mehdipour,[2,3] B. T. Goh,[1] and S. A. Rahman[1]
[1]*Low Dimensional Materials Research Centre, Department of Physics, Faculty of Science, University of Malaya, 50603 Kuala Lumpur, Malaysia*
[2]*Plasma Nanoscience Centre Australia (PNCA), CSIRO Materials Science and Engineering, P.O. Box 218, Lindfield, New South Wales 2070, Australia*
[3]*Plasma Nanoscience @ Complex Systems, The University of Sydney, New South Wales 2006, Australia*

(Received 23 April 2013; accepted 18 June 2013; published online 8 July 2013)

Using numerical modeling of the plasma sheath and key surface processes, the plasma-aided fabrication of InAs nanodots is investigated at early stage of the growth. Roles of different plasma process parameters, such as electron temperature, electron number density, and ion-to-electron density ratio, in achieving the stoichiometric growth of the nanodots are explored and conditions to achieve a highly stoichiometric InAs composition are discussed. It is shown that the nanodots get larger with increasing the electron temperature and electron number density, whereas they shrink in size with increasing the ion-to-electron density ratio. Moreover, it is shown that with increase in the electron temperature and electron number density stoichiometric saturation state can be reached shortly, which this enables the fabrication of highly stoichiometric array of nanodots within shorter processing time. The results obtained can open a path toward nucleation and growth of an array of nanodots with desired structural composition and size distribution. [http://dx.doi.org/10.1063/1.4813116]

I. INTRODUCTION

Among III-V semiconductors, indium arsenide nanostructures have found numerous applications in optics[1] thermophotovoltaics,[2] high-speed electronics,[3] micro-, photo- and nanoelectronics[4,5] due to its narrow band gap and high electron mobility as well as the ohmic contact of many metals with InAs.[6–10] Among them are mid-wave infrared and long-wave infrared detectors, light emitting diodes, lasers diode, heterojunction bipolar transistors, and high electron mobility transistors as well as biological sensor.

Although numerous techniques have been developed in order to fabricate well-ordered arrays of InAs,[11–16] growing highly stoichiometric ([In]/[As] = 1:1) nanodots (NDs) is still challenging. Studies show that the stability and optical properties of NDs strongly depend on surface structure and composition of the nanostructure.[17] In other words, a non-stoichiometric composition ([In]/[As] ≠ 1:1), even if the deviation is very small, causes unwanted defects in the nanostructures and thus undesirably affects quality and performance of ND devices. Therefore, it is of importance to obtain a ratio of In to As 1:1 for the entire ND structure, from the inner core to the outmost layer.

The importance of obtaining a stoichiometric composition for arrays of NDs has led to many studies in recent years.[18,19] Rider *et.al*[18] investigated the growth of SiC quantum dots (QDs) and found that two key factors play crucial role in determining time-dependent behavior of Si to C adatom ratio: (1) substrate surface temperature and (2) the ratio of Si to C atom/ion influx to the substrate. In another word, it is found that self-assembling of highly-stoichiometric SiC QDs is possible if only a specific combination of these two factors is selected. By comparing different neutral/ionized gas conditions, they also showed that the stoichiometric state can be reached within shorter time periods when plasma is used as the growth environment.[19]

Plasma is a suitable environment for pretreatment and synthesis as well as postgrowth processing of nanomaterials of a broad range of the elements. Plasma-aided processes, due to the significant role of plasma in generation, control, transport and deposition of the building units, are quite efficient for the growth of NDs.[20–22] All the nanostructures grown on plasma-exposed substrate in fact are assembled in plasma sheath which is formed adjacent to the substrate and controls the dynamic of charge species[23] (ions and electrons) which are contributing in heating[24] and the growth of nanostructures. The plasma sheath characteristics, such as sheath thickness, strongly depends on the plasma process parameters at the boundary between sheath and the plasma bulk (sheath edge), such as electron temperature T_e, electron number density n_{e0}, and number density ratio of the ions to electrons f.[23,25]

In this work, using self-consistent numerical solution of the plasma sheath and surface rate equations, we studied the effect of variations in these plasma process parameters on the plasma-induced substrate heating and growth of binary III-V NDs (InAs NDs studied here). Required ionized gas conditions to obtain highly stoichiometric composition of the InAs NDs, at early stage of growth are presented and discussed. In fact, we will show how plasma effects can enable fast growth of stoichiometric InAs NDs at low temperatures.

The paper is structured as follows. In the Sec. II, the main assumption of the plasma sheath and numerical model of InAs NDs growth and main equations involved are

presented. The result of numerical study of the effect of the sheath parameters on surface fluxes of In and As adsorbed ions and elemental composition and size distribution of InAs NDs are presented and discussed in Sec. III. Finally, the main findings of this work are summarized in Sec. IV.

II. MODEL AND BASIC EQUATIONS

Plasma sheath of a four-fluid plasma consisting of electrons and In^+, As^+, and Ar^+ ions is considered. We assume that the plasma sheath along x and y direction is homogenous and thus variations of the physical properties are considered in the z direction perpendicular to the substrate (see Fig. 1(a)). The governing equations[23,26] are continuity

$$\frac{d}{dz}(n_{ij}\upsilon_{ijz}) = \nu_{Ij}n_e, \tag{1}$$

$$\frac{d}{dz}(n_e\upsilon_{ez}) = n_e\sum_j \nu_{Ij}, \tag{2}$$

and momentum equations

$$m_{ij}\upsilon_{ijz}\frac{d\upsilon_{ijx}}{dz} = -m_{ij}\nu_{ijn}\upsilon_{ijx}, \tag{3}$$

$$m_{ij}\upsilon_{ijz}\frac{d\upsilon_{ijy}}{dz} = -m_{ij}\nu_{ijn}\upsilon_{ijy}, \tag{4}$$

$$m_{ij}\upsilon_{ijz}\frac{d\upsilon_{ijz}}{dz} = -e\frac{d\phi}{dz} - \frac{T_{ij}}{n_{ij}}\frac{dn_{ij}}{dz} - m_{ij}\nu_{ijn}\upsilon_{ijz}, \tag{5}$$

$$0 = e\frac{d\phi}{dz} - \frac{T_e}{n_e}\frac{dn_e}{dz} - m_e\nu_{en}\upsilon_{ez}, \tag{6}$$

for j-type ions ($j=1$, 2, 3 represents In, As, and Ar ions, respectively) and electrons. In above equations, m_{ij} is the mass, n_{ij} is the number density, υ_{ijx}, υ_{ijy}, and υ_{ijz} are the x, y, and z components of the fluid velocities of j-type ion and ϕ,

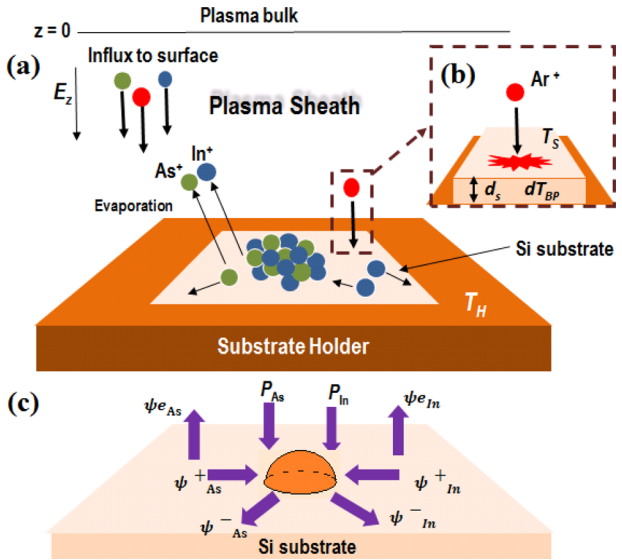

FIG. 1. (a) Schematic of the plasma sheath and InAs nanodots growth on silicon surface, (b) plasma heating process, and (c) fluxes of ions and adsorbed ions to/from the nanodot.

T_e, T_{ij}, and υ_{ex} are electric potential, electron temperature, j-type ion temperature, and x component of the electron velocity, respectively. Furthermore, ν_{Ij}, ν_{ijn}, and ν_{en} are the ionization frequency (of j-type ions), the j-type ion-neutral collision frequency, and electron-neutral collision frequency, respectively. Here, we assumed the following parameters as the default parameters:[23,26,27]

$$T_{i\mathrm{In}} = 0.1\,\mathrm{eV}, \quad T_{i\mathrm{As}} = 0.05\,\mathrm{eV}, \quad T_{i\mathrm{Ar}} = 0.05\,\mathrm{eV},$$
$$\nu_{I\mathrm{In}} = 0, \quad \nu_{i\mathrm{In}n} = 0.1\omega_{pi\mathrm{In}}, \quad \nu_{I\mathrm{As}} = 0, \quad \nu_{i\mathrm{As}n} = 0.1\omega_{pi\mathrm{As}},$$
$$\nu_{I\mathrm{Ar}} = 0.1\omega_{pi\mathrm{Ar}}, \quad \nu_{i\mathrm{Ar}n} = 0.1\omega_{pi\mathrm{Ar}},$$
$$\nu_{en} = 0.00001 m_e\omega_{pij}/m_j,$$

where $\omega_{pij}(\propto m_j^{-1/2})$ is the plasma frequency of j-type ions. In this work, the ion temperature and total gas pressure are taken constant. Therefore, the ion/electron-neutral collision frequencies assumed constant and have been set to reasonably-evaluated values that properly represent ion/electron-neutral collision conditions in a typical low-pressure weakly ionized plasma environment currently utilized in plasma-aided synthesis of nanomaterials.[20] Furthermore, since the Ar ion plasma frequency $\omega_{pi\mathrm{Ar}}$ is much larger than As and In ionization frequencies, $\nu_{I\mathrm{As}}$ and $\nu_{I\mathrm{In}}$, (due to $m_{Ar} < m_{In/As}$), $\nu_{I\mathrm{As}}$ and $\nu_{I\mathrm{In}}$ been assumed zero.

Electric potential is obtained from the one-dimensional Poisson equation

$$\frac{d^2\phi}{dz^2} = 4\pi e\left(n_e - \sum_j n_{ij}\right). \tag{7}$$

We assumed that at the sheath edge for an undisturbed plasma, the quasineutrality condition is satisfied, i.e.,

$$n_{e0}e\left(1 - \sum_j f_j\right) = 0, \tag{8}$$

where $f_j = n_{ij0}/n_{e0}$ is the number density ratio of j-type ions to electrons at $z=0$ (plasma-sheath boundary).

The set of above equations is supplemented by the following boundary conditions at the sheath edge ($z=0$):

$$\upsilon_{i\mathrm{In}z} = 1.5c_{si\mathrm{In}}, \quad \upsilon_{i\mathrm{As}z} = 1.5c_{si\mathrm{As}}, \quad \upsilon_{i\mathrm{Ar}z} = 2.0c_{si\mathrm{Ar}},$$
$$\phi = 0, \quad \partial\phi/\partial z = 0.01/\lambda_{De}.$$

Here, $c_{sij} = \sqrt{T_e/m_i}$ and $\lambda_D = \sqrt{(K_BT_e)/(4\pi e^2 n_e)}$ are the j-type ion-acoustic velocity and electron Debye length, respectively. The selected small potential difference at the sheath edge reflects the fact that there exists a very weak electric field at the plasma-sheath boundary due to existence of so-call (quasineutral) pre-sheath region across which the ions are accelerated up to the speeds typically larger than ion-acoustic velocity.[28]

In order to solve the above set of equations, Eqs. (1)–(8), we first normalized the equations,[23,26] then the set of normalized equations is solved using a fourth-order-Rung-Kutta method. By solving the equations, the influxes of In and As ions (at substrate), $P_{\mathrm{In}} = n_{i\mathrm{In}}\upsilon_{i\mathrm{In}z}$ and $P_{\mathrm{As}} = n_{i\mathrm{As}}\upsilon_{i\mathrm{As}z}$ as well as the energy and flux of bombarding Ar ions are

obtained and then used as input parameters in the models of plasma-enabled heating and ND growth.

Increase in the substrate temperature due to Ar ion bombardment dT_{BP} in plasma is obtained from the following equation:[29]

$$dT_{BP} = (n_{Ar^+}\varepsilon_{Ar^+}\upsilon_{Ar^+})d_s/\chi_s, \quad (9)$$

where d_s, χ_s, and ε_{Ar+} are substrate diameter, Si thermal conductivity and energy of Ar ions, respectively. A very simple schematic of the energy release is sketched in Fig. 1(b). Equation (9) describes the energy released to the substrate surface (exposed to the plasma) and consequently the temperature rise at the Si top surface respect to the substrate-substrate holder interface. In this work, as we study ND growth in low temperature range (unique to plasma-aided fabrication of ND arrays)[20] and the default parameters are set for low pressure case, we take into account only the role of the ion bombardment in energy exchange between the ionized gas and substrate. There are definitely energy loss processes, such as thermal radiation and convection, which are effective in the processes where the substrate temperature and gas pressure are relatively high (e. g., chemical vapor deposition).[29] Using $T_s = T_H + dT_{BP}$, we can obtain real substrate temperature, T_s, when the substrate holder is heated externally to T_H.

The model of ND growth is based on a set of rate equations which describes the time evolution of surface density of ND (with different numbers of building blocks) and stoichiometric factor as well as distribution of ND sizes under various ionized gas conditions.[30,31] In this case, as it can be seen in Fig. 1(c), a large number of key surface processes contributing to ND growth, such as As/In surface diffusion, attachment and detachment (into the ND structure) as well as evaporation (from the substrate surface), are taken into account. Here, we assume that the substrate surface is a flat and smooth surface area and the atoms can freely diffuse on it as they gain enough thermal energy. The moving atoms reach to each other and form initial nucleation sites to which the next coming atoms attach (or detach as time advances). The rate equations for In and As ions are

$$\frac{\partial \eta_{In}}{\partial t} = P_{In} - \psi^e_{In} + \sum_{i=2}^{\infty} n_{In.i}\eta_i\mu_{In.i} - \eta_{In}\sum_{i=2}^{\infty}\sigma_i\eta_i\upsilon_{d.In} - 2\sigma_1{\eta_{In}}^2\upsilon_{d.In} - \sigma_1\eta_{In}\eta_{As}\upsilon_{d.In}, \quad (10)$$

$$\frac{\partial \eta_{As}}{\partial t} = P_{As} - \psi^e_{As} + \sum_{i=2}^{\infty} n_{As.i}\eta_i\mu_{As.i} - \eta_{As}\sum_{i=2}^{\infty}\sigma_i\eta_i\upsilon_{d.As} - 2\sigma_1{\eta_{As}}^2\upsilon_{d.As} - \sigma_1\eta_{In}\eta_{As}\upsilon_{d.As}, \quad (11)$$

where η_i is the surface density of the NDs; $n_{\mathrm{In}.i}$ and $n_{\mathrm{As}.i}$ are numbers of In and As atoms at the borders of the NDs consisting i-atoms; $\mu_{\mathrm{In}.i}$ and $\mu_{\mathrm{As}.i}$ are the frequency of In and As atom re-evaporation from the borders of (i)-atom NDs; σ_i is the diameter of (ML) NDs. Here, $\psi^e_{\mathrm{In(As)}} = n_k\nu_0 \exp(-\varepsilon_{a.\mathrm{In(As)}}/KT)$, and $\upsilon_{d.\mathrm{In(As)}} = \lambda\nu_0\exp(-\varepsilon_{d.\mathrm{In(As)}}/KT)$ are flux of In/As evaporation (from the substrate surface) and linear surface velocity of In/As ions, respectively. As reflected in the evaporation rate expression, the evaporation of In and As atoms, which have been chemisorbed on the surface, is a thermally activated process which takes place when As/In atom acquire enough thermal energy (to break the bond between them and substrate neighboring atoms).

The rate equations for i-atom NDs is

$$\frac{\partial \eta_i}{\partial t} = \sigma_{i-1}\eta_{i-1}(\eta_{In}\upsilon_{d.In} + \eta_{As}\upsilon_{d.As}) - \sigma_i\eta_i(\eta_{In}\upsilon_{d.In} + \eta_{As}\upsilon_{d.As}) + \eta_{i+1}n_{i+1}(\mu_{In.(i+1)} + \mu_{As.(i+1)}) - \eta_i n_i(\mu_{In.i} + \mu_{As.i}). \quad (12)$$

Using Eq. (12), the ratio of net fluxes of In and As ions to the ND boundary, the stoichiometric factor, is defined as[18]

$$k_{st}(t) = \sum_{i=2}^{N}[(\eta_{In}\upsilon_{d.In}\sigma_i\eta_i - \eta_i n_i\mu_{In.i})/(\eta_{As}\upsilon_{d.As}\sigma_i\eta_i - \eta_i n_i\mu_{As.i})], \quad (13)$$

where N is the maximum number of atoms forming a ND. It must be mentioned that as we are study the early stage of ND growth, i. e., the nucleation stage, which takes place in short time periods (in order of a fraction of second) and dictates the evolution of ND structure at the later stage, the maximum number of atoms N has to be small enough (e. g., $N = 120$ as considered here). Correspondingly, studying nucleation phenomenon for very small-size NDs in long time periods is not physically reasonable. A list of parameters used in this work is presented in Table I. In this model, the ion energies and fluxes are highly dependent on the characteristics of the plasma sheath (i.e., the sheath thickness), which is in turn influenced by the plasma parameters at the sheath edge (electron temperature, T_e, electron density, n_{e0}, and ion-to-electron number density ratio, f). The plasma process parameters and thus the substrate temperature were varied in our numerical calculations to observe effects of change of the sheath characteristics on the structure and composition of InAs NDs.

III. RESULTS AND DISCUSSION

In this section, the results of solutions of the sheath and the ND growth equations from Sec. II are presented and discussed. Using these solutions, the dependencies of

TABLE I. Parameters and representative values of the simulation.

Parameter	Value	Reference
Physical constants		
Lattice parameter, λ	5×10^{-10} m	29
Lattice atom oscillation frequency, ν_0	1×10^{13} s^{-1}	30
In atom diffusion activation energy, $\varepsilon_{d.\mathrm{In}}$	0.71 eV	19
In atom evaporation activation energy, $\varepsilon_{a.\mathrm{In}}$	2.85 eV	19
As atom diffusion activation energy, $\varepsilon_{d.\mathrm{As}}$	0.41 eV	19
As atom evaporation activation energy, $\varepsilon_{a.\mathrm{As}}$	1.64 eV	19
Si thermal conductivity, χ_s	78 Wm^{-1}K^{-1}	31
Simulation parameters		
Surface coverage, η	0–0.5 monolayers (ML)	
Maximum number of atoms in nanodots, N	120	
Substrate holder temperature, T_H	500 K	
Time of deposition, t	0–20 ms	

stoichiometric factor (k_{st}) and surface coverage (η_i) of InAs NDs on plasma parameters (i.e., electron temperature (T_e), electron density, n_{e0}, and number density ratio of ions to electrons, f) are described with an emphasis on the effects of the parameters on the substrate temperature.

Figure 2(a) displays the stoichiometric factor, k_{st}, as a function of time for different electron temperatures. It is clearly seen that, at low electron temperatures (here $T_e = 1$ eV), k_{st} can only reach to an unsaturated value of 0.8 (at the end of the process), whereas it saturates at near-stoichiometric level of 0.97 after process time of 10 ms for a moderate electron temperature of 1.8 eV. With further increase in the temperature, the stoichiometric saturation time decreases. This can be explained by considering the effect of electron temperature change on the sheath characteristics and the surface temperature. When the electron temperature T_e is increased more intense fluxes of As and In ions are generated (due to more effective ionization processes) and then flow towards the substrate. Besides, the plasma sheath thickness increases with increasing the electron temperature which gives rise to ions species gaining more kinetic energy when they travel through the sheath width. Consequently, much larger amount of energy is released to the substrate surface due to effective bombardments by more energetic ions, which in turn gives rise to an increase in surface temperature (with respect to the substrate holder). The numerical solution suggests a surface temperature increase in above 50 K (from 536 to 588 K) due to an increase in electron temperature from 1 to 1.8 eV. As a result of surface temperature increase and more intense fluxes of In and As ions (to the substrate surface), the process of ND formation is accelerated, thus stoichiometric state is reached within shorter time periods. However, as Fig. 2(a) suggests, care must be taken when increasing the electron temperature since any extra increase in T_e may lead to uncontrolled building units supply (of ND growth) and eventually formation of non-stoichiometric NDs.

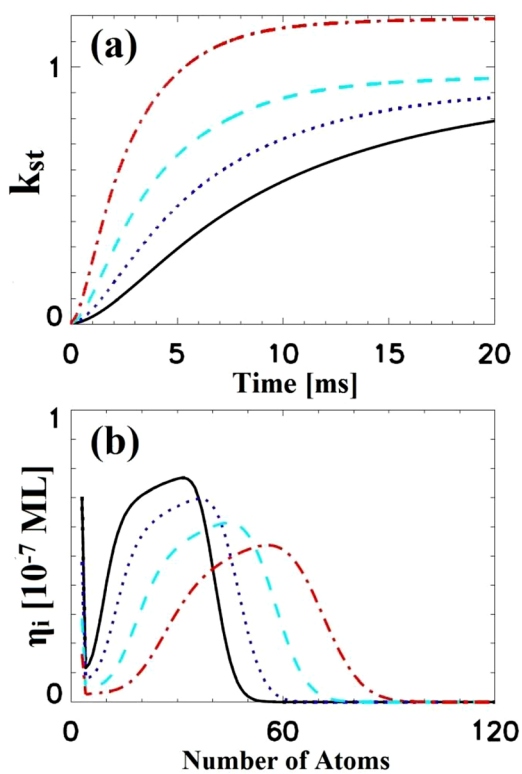

FIG. 2. Time evolution of the adsorbed ion balance factor k_{st} (a) and size distribution of the nanodots η_i (b) for different electron temperatures T_e. Solid, dotted, dashed, and dashed-dotted curves correspond to $T_e = 1$ eV, 1.4 eV, 1.8 eV, and $T_e = 2.2$ eV, respectively.

Figure 2(b) illustrates the dependence of surface density of i-atomic NDs on the number of atoms with the same parameters as in Fig. 2(a). For all electron temperatures, η_i starts from a high amount and after a quick drop, rise again and reaches its maximum value, then decreases and eventually becomes zero. The decrease in the density and becoming nearly zero at large atom numbers reflects the fact that nucleation of extremely large NDs is very unlikely to happen within very short time periods (studied here) and such large size ND can only form by attachment of more atoms into structure of as-nucleated small NDs. For $T_e = 1$ eV, the highest surface density of NDs is obtained at $i = 35$ atoms. As a comparison, for $T_e = 2.2$ eV, maximum value of η_i is occurred at $i = 60$ atoms. Thus, the increase in electron temperature causes the InAs NDs density to shift to higher number of atoms and bigger NDs with lower densities are obtained. Such an effect is possibly attributed not only to higher influx from the plasma environment at higher electrons temperature. As mentioned above, with increasing the electron temperature, the plasma sheath thickness increases and as a result the Ar ions gain more kinetic energy while they travel across the sheath. Hence, more effective collisions of the ions at the substrate give rise to (release of higher amounts of energy at the substrate surface and therefore) a remarkable increase in substrate temperature and growth of larger NDs. This is consistent with the experimental reports of increase in the ND size with increasing the temperature.[32–38]

Let us now examine the dependence of balance factor k_{st} on time at different number ratios of Ar ions to electrons at plasma sheath edge, f (Fig. 3(a)). It can be clearly observed from Fig. 3(a) that by increasing f, the saturation level of stoichiometric factor climbs up, but no major changes can be identified in the time to reach the saturation level. This can be clarified via recalling the quasineutrality equation (Eq. (8)) binding directly number densities of Ar, In, and As ions at plasma sheath edge ($z = 0$). As can be understood from Eq. (8), there is an inverse relationship between n_{Ar^+0} and $n_{In^+0} + n_{As^+0}$. Hence, with an increase in Ar ion number density at plasma sheath edge, the total influx which contributes to growth process of InAs NDs decreases dramatically. For $f = 0.65$, substrate temperature and total influx are $T_s = 569$ K and $P^+ = 13.3$ ML s^{-1}, respectively. As f increases to 0.85, these values become 586 K and 5.7 ML s^{-1}, respectively. Therefore, although the substrate temperature rises with increasing the Ar ion number density, it is accompanied with a decrease in the total building units influx on which the growth outcome and elemental composition of InAs NDs critically depend.[18] Dependence of surface density of i-atomic NDs on number of atoms with the same parameters as Fig. 3(a) is plotted in Fig. 3(b). The peaks of the NDs surface

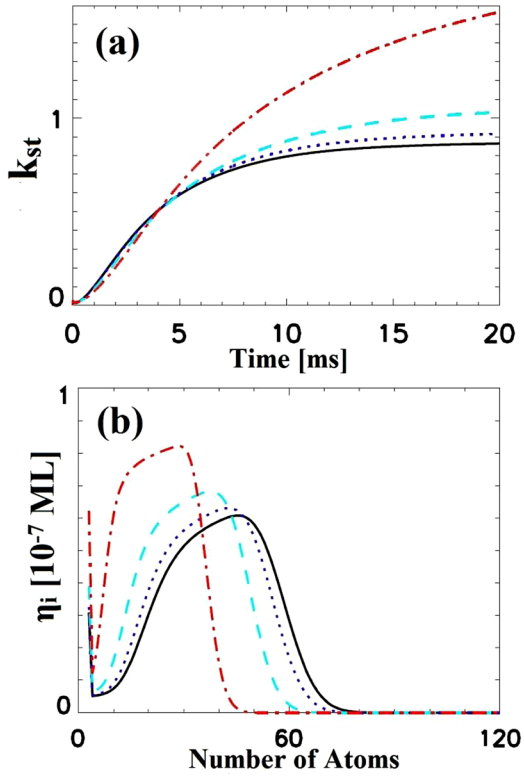

FIG. 3. Time evolution of the adsorbed ion balance factor k_{st} (a) and size distribution of the nanodots η_i (b) for different ion-to-electron density ratios f. Solid, dotted, dashed, and dashed-dotted curves correspond to $f = 0.65$, 0.75, 0.85, and $f = 0.95$, respectively.

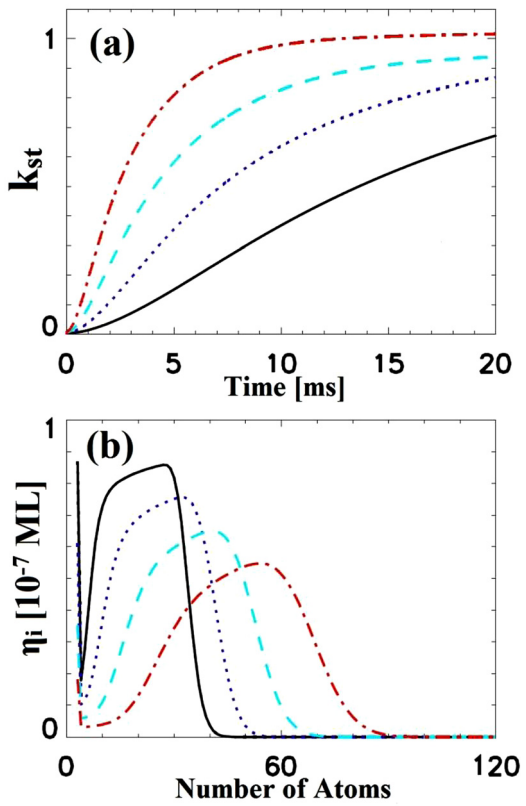

FIG. 4. Time evolution of the adsorbed ion balance factor k_{st} (a) and size distribution of the nanodots η_i (b) for different electron number densities n_{e0}. Solid, dotted, dashed, and dashed-dotted curves correspond to $n_{e0} = 1.5 \times 10^{10}\,\mathrm{cm}^{-3}$, $3.0 \times 10^{10}\,\mathrm{cm}^{-3}$, $4.5 \times 10^{10}\,\mathrm{cm}^{-3}$, and $n_{e0} = 6.0 \times 10^{10}\,\mathrm{cm}^{-3}$, respectively.

density for $f = 0.65$, 0.75, 085, and 0.95 are obtained at $i = 45$, 43, 38, and 33, respectively. Hence, in contrast to Fig. 2(b), here, the increase in Ar ion density causes the peak of InAs NDs density to move towards lower number of atoms. As mentioned above, this is because the total flux of generated ions decreases with increasing the ion-to-electron density ratio f.

Nucleation and growth of NDs strongly depend on temperature and the surface densities of building blocks which both are tightly dependent on the fluxes and energies of species from the plasma sheath. Figure 4(a) displays the time-dependence behavior of k_{st} at different values of electron density at the sheath edge. The general tendency is that as electron density increases, the saturation level of k_{st} is reached in shorter time. Therefore, higher electron densities at the sheath edge cause faster stoichiometrization of InAs NDs. At higher electron densities, the sheath thickness becomes smaller. Accordingly, one may expect that there should be an opposite trend as shown in Fig. 1(a) where the sheath thickness becomes wider with increasing the electron temperature. But as electron density increases, a very strong electric field is generated due to a sharp decrease in the sheath thickness. Thus, the substrate surface is actually exposed to larger influxes of much more energetic ions and the plasma-assisted heating of the substrate surface is further enhanced. Our calculations shows that the surface temperature corresponded to $n_{e0} = 1.5 \times 10^{10}\,\mathrm{cm}^{-3}$ is 526 K while for $n_{e0} = 6 \times 10^{10}\,\mathrm{cm}^{-3}$ which results in $k_{st} = 1$, surface temperature reaches to 605 K. Therefore, electron density has a significant effect on substrate temperature and time period to reach stoichiometric state can be adjusted by simply changing the electron density at the sheath edge (plasma density). Similar tendency as Fig. 2(b) is seen for η_i with different values of n_{e0} (Fig. 4(b)). Thus, as interpreted above, increase in electrons density at $z = 0$ results in formation of larger NDs. The trends obtained numerically in Figs. 2(b) and 4(b) are in good agreement with the experimental results of Cheng *et al.*[35] and Huang *et al.*[36] who reported increase in average size of NDs with plasma parameters and substrate temperature.

Now, we consider dependence of stoichiometric factor of absorbed ions on electron temperature at different times of ND growth process with the number density ratio of Ar ions to electrons (f) as the parameter (Fig. 5). The first observation is that, over short time periods (Fig. (5)), in the low electron temperature range ($T_e < 1.6\,\mathrm{eV}$), the influx of As ions is always larger than that of In ions (i.e., k_{st} is lower than 1) and increase in f does not raise level of the balance factor. In other words, when the electron temperature is low, for short time periods the stoichiometric state ([In]/[As] = 1:1) is never obtained by varying (increasing) the Ar ion density (at plasma sheath edge). However, by increasing the electron temperature, the stoichiometric state is achieved still at high Ar ion densities. Therefore to achieve a stoichiometric state during short processing time periods, it is necessary that electron temperature is higher than a threshold value and Ar ion density is kept high enough.

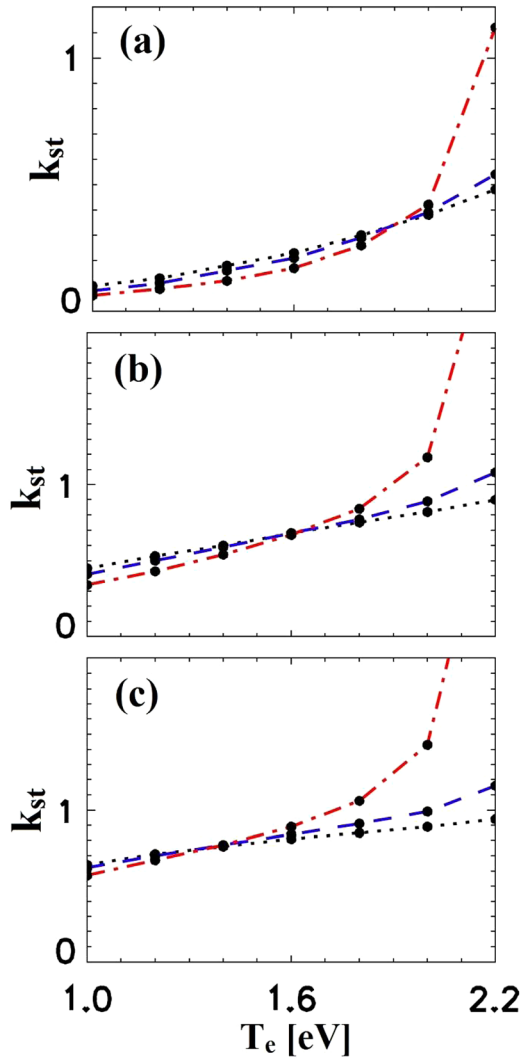

FIG. 5. Dependence of absorbed ion balance factor k_{st} on electron temperature for an ion-to-electron density ratio of $f=0.7$ (dotted), $f=0.8$ (dashed), $f=0.9$ (dashed-dotted), and for a process time period of (a) 2 ms, (b) 7 ms, (c) 12 ms.

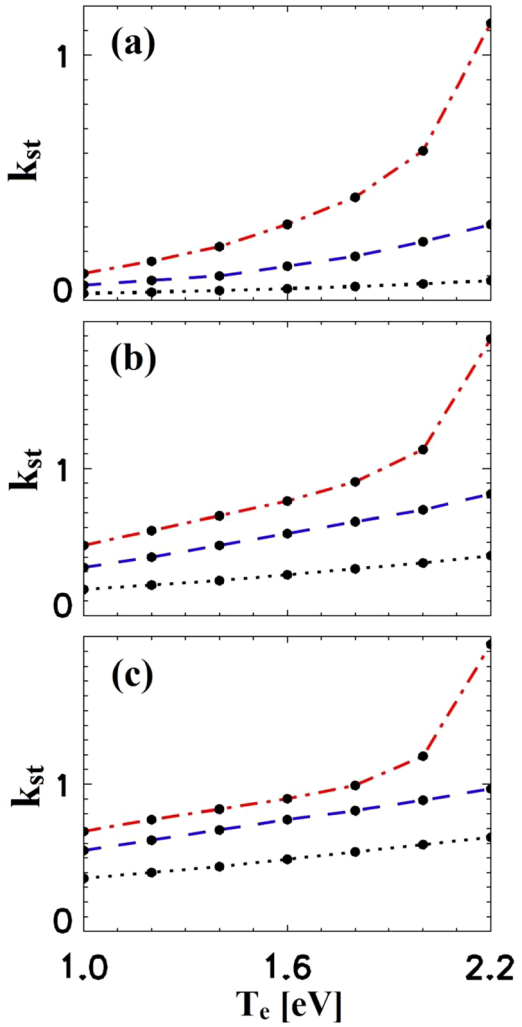

FIG. 6. Dependence of flux balance factor k_{st} on electron temperature for an electron number density of $n_{e0}=2.0\times10^{10}\,\mathrm{cm}^{-3}$ (dotted), $n_{e0}=4.0\times10^{10}\,\mathrm{cm}^{-3}$ (dashed), $n_{e0}=6.0\times10^{10}\,\mathrm{cm}^{-3}$ (dashed-dotted), and for a process time period of (a) 2 ms, (b) 7 ms, (c) 12 ms.

However, as can be clearly observed in Figs. 5(b) and 5(c), for longer processing time periods, even at low electron temperature, the stoichiometric state can be reached by increasing the Ar ion density (increasing f). In fact, as Fig. 5 suggests, the stoichiometric state of InAs NDs growth can be obtained by simply adjusting f and T_e, and growth time parameter at some specific values. For example, for process time periods of $t=2$ ms and 7 ms, $k_{st}=1$ is obtained for $f=0.9$, $T_e=2.19$ eV and $f=0.9$, $T_e=1.9$ eV, respectively, whereas for $t=12$ ms this state is occurred in two cases: (i) $f=0.8$, $T_e=2.0$ eV and (ii) $f=0.9$, $T_e=1.75$ eV.

To further clarify the effect of electron density on the process, we have plotted dependence of k_{st} on electron temperature at different times of ND growth process with electron density at z = 0 as the parameter in Fig. 6. It is clearly seen that except for the range of higher electron temperatures and densities, k_{st} is a linear function of the electron temperature and the slope increases with the process time period. Despite f (Fig. 5), here in the low electron temperature range, increase in n_{e0} remarkably enhances stoichiometric factor of In and As absorbed ions. However, in the range of $T_e<1.6$ eV, influx of As ions to the substrate is larger than that of In and a highly nonstoichiometric (Arsenic-rich) state is occurred. The unbalanced state is also observed for higher electron temperatures and densities but here influx of In ions is larger than that of As (indium-rich state). As Fig. 6 suggests, one way to mediate these unbalanced influxes of In and As adsorbed ions at the early stage of the growth of InAs NDs is to temporarily increase electron density for Arsenic-rich state and to decrease electron temperature for Indium-rich state. In brief, similar to Fig. 5, in Fig. 6 also a simultaneous optimization can be used in order to make the stoichiometrization process more quickly.

Finally, Fig. 7 illustrates dependence of stoichiometric factor of InAs NDs on n_{e0} for different process time periods with the number density of Ar ions as the parameter. The general trend is the same as Fig. 5. For the process time period of t = 2 ms (Fig. 7(a)), the three curves are overlapped at a low level and by increasing in f no major changes can be identified up to $n_{e0}=7\times10^{10}\,\mathrm{cm}^{-3}$. In this range, the maximum value of k_{st} equals to 0.65 which is obtained for

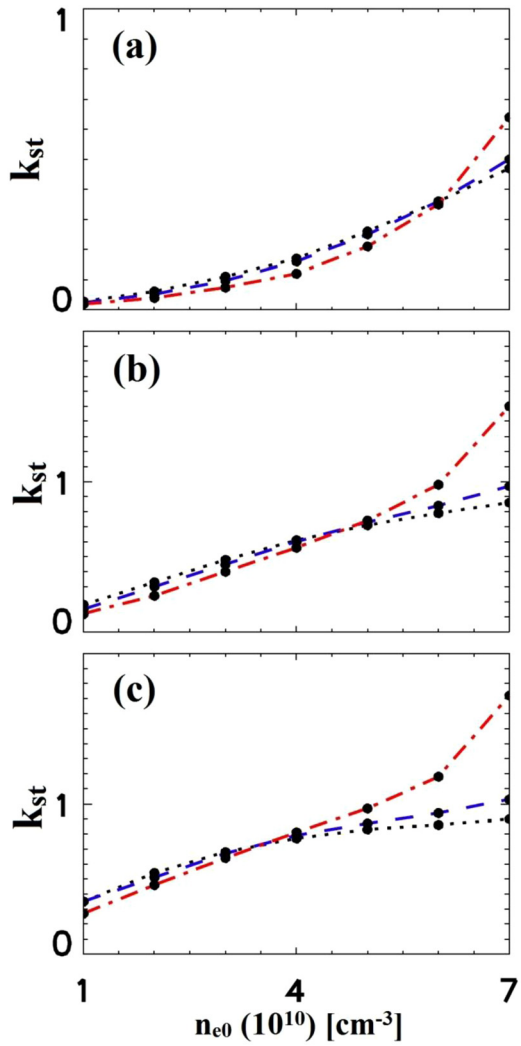

FIG. 7. Dependence of stoichiometric factor k_{st} on n_{e0} for an ion-to-electron density ratio of $f=0.7$ (dotted), $f=0.8$ (dashed), $f=0.9$ (dashed-dotted), and for a process time period of (a) 2 ms, (b) 7 ms, (c) 12 ms.

$n_{e0}=7\times10^{10}\,\mathrm{cm}^{-3}$ and $f=0.9$. Figure 7(a) documents that over the short time periods (considered here) in the near-low electron temperature range ($T_e<1.7$ eV), it is not possible to grow stoichiometric NDs even by simultaneous increasing of both n_{e0} and f. This unwanted state improves unambiguously for the subsequent process time periods and is only observed for smaller values of n_{e0}. However, one can see from Figs. 7(b) and 7(c) that stoichiometric state occurs for different sets of values considered for the parameters of n_{e0} and f. As a result, to achieve and maintain a stoichiometrical composition of InAs NDs, optimal values of n_{e0} and f should be selected and the optimal values vary for different process time periods.

IV. CONCLUSION

In this work, we investigated growth process of InAs NDs on Si(100) surface in a plasma environment at early stage of growth. Our objectives were to study effects of the background gas parameters on influx of absorbed In and As ions as well as on substrate surface heating for the purpose of achieving a stoichiometric state for InAs NDs at the earliest possible time when the structure is at its smallest. Numerical simulation results are summarized as follows:

- the surface processes (i.e., building block attachment/detachment to/from the NDs, evaporation, etc.) are effectively tuned by variation of plasma sheath parameters. Therefore, the entire ND growth process, nucleation, and growth of NDs, distribution of ND sizes built as well as elemental composition of NDs can be effectively controlled by simply adjusting the plasma process parameters, namely, electron temperature, plasma density (electron density at the sheath edge), and the number density ratio of argon ions to electrons. Besides, more importantly, understanding effect of the plasma sheath dynamics on substrate surface temperature and the net surface flux of In and As ions to InAs NDs can promisingly provide a way to obtain highly-stoichiometric NDs at initial stage of their self-assembly;
- in particular, increasing the electron temperature and electron density at the sheath edge due to the direct effect on surface temperature results in faster stoichiometrization of InAs NDs. However, to avoid non-stoichiometric NDs, these parameters should be increased to a certain threshold;
- by rising the number density ratio of Ar^+ to electron at the sheath edge, the substrate temperature increases and simultaneously the total influx of ions decreases. These effects raise the saturation level of k_{st} but no major changes can be identified in the time to reach the saturation level;
- with the increase in electron temperature and electron density at the sheath edge, the maximum value of NDs surface density is obtained for higher number of atoms. This means that bigger NDs are grown. Whereas for the parameter of $(n_{Ar}{}^{+}/n_e)_{z=0}$, the reverse situation is observed;
- one promising way to mediate unbalanced influxes of In and As adsorbed ions in the growth of InAs NDs is to temporarily increase electron density and to decrease electron temperature for Arsenic-rich and Indium-rich states, respectively;
- slope of stoichiometric factor plot versus T_e becomes steeper by increasing n_{e0} and stoichiometric factor of absorbed ions shifts to higher values; and
- by choosing specific combination of plasma parameters growth of highly stoichiometric NDs is possible within shortest possible time periods.

The results presented here can open a path toward dynamical control of nanoassembly processes, and thus, nucleation and growth of an array of NDs with desired structural composition and size distributions. In this work, we neglected the effect of externally applied magnetic field or presence of nanosize dust grains (i.e., dusty plasma) on stoichiometric growth of InAs NDs and are left for future works.

ACKNOWLEDGMENTS

This work was supported by University of Malaya postgraduate research Fund (PPP) of PG081-2012B and high impact research (HIR) Fund of MOHE-HIR F000006-21001.

H.M. also acknowledges the support by the University of Sydney International Scholarship and CSIRO OCE top-up scholarship.

[1]B. L. Liang, Z. M. Wang, Yu. I. Mazur, G. J. Salamo, E. A. Decuir, Jr., and M. O. Manasreh, Appl. Phys. Lett. **89**, 043125 (2006).
[2]L. M. Fraas, G. R. Girard, J. E. Avery, B. A. Arau, V. S. Sundaram, A. G. Thompson, and J. M. Gee, J. Appl. Phys. **66**, 3866 (1989).
[3]C. R. Bolognesi, J. D. Werking, E. J. Caine, H. Kroemer, and E. L. Hu, IEEE Electron Device Lett. **14**, 13 (1993).
[4]B. Cakmak, Opt. Express **10**, 530 (2002).
[5]M. Walther, R. Rehm, F. Fuchs, J. Schmitz, J. Flei, W. Cabanski, D. Eich, M. Finck, W. Rode, J. Wendler, R. Wollrab, and J. Ziegler, J. Electron. Mater. **34**, 722 (2005).
[6]A. Trampert, E. Tournie, and K. H. Ploog, J. Cryst. Growth **146**, 368 (1995).
[7]S. E. Hooper, D. I. Westwood, D. A. Woolf, S. S. Heghoyan, and R. H. Williams, Semicond. Sci. Technol. **8**, 1069 (1993).
[8]S. Kalem, J. Appl. Phys. **66**, 3097 (1989).
[9]S. Kalem, Semicond. Sci. Technol. **5**, S200 (1990).
[10]Z. M. Fang, K. Y. Ma, R. M. Cohen, and G. B. Stringfellow, Appl. Phys. Lett. **59**, 1446 (1991).
[11]H. Naoi, D. M. Shaw, G. J. Collins, and S. Sakai, J. Cryst. Growth **219**, 481(2000).
[12]H. H. Zhan, R. N. Notzel, G. J. Hamhuis, T. J. Eijkemans, and J. H. Wolter, J. Cryst. Growth **251**, 135 (2003).
[13]J. Shi, K. Zhu, W. Yao, and L. Zhang, J. Cryst. Growth **186**, 480 (1998).
[14]P. Thilakan, Z. Iqbal kazi, and T. Igawa, Appl. Surf. Sci. **191**, 196 (2002).
[15]T. Alzoubi, M. Usman, M. Benyoucef, and J. P. Reithmaier, J. Cryst. Growth **323**, 422 (2011).
[16]M. Innocenti, F. Forni, G. Pezzatini, R. Raiteri, F. Loglio, and M. L. Foresti, J. Electroanal. Chem. **514**, 75 (2001).
[17]F. A. Reboredo, L. Pizzagalli, and G. Galli, Nano Lett. **4**, 801 (2004).
[18]A. E. Rider, I. Levchenko, and K. Ostrikov, J. Appl. Phys. **101**, 044306 (2007).
[19]A. E. Rider and K. Ostrikov, Surf. Sci. **603**, 359 (2009).
[20]K. Ostrikov, Rev. Mod. Phys. **77**, 489 (2005).
[21]I. Levchenko, K. Ostrikov, K. Diwan, K. Winkler, and D. Mariotti, Appl. Phys. Lett. **93**, 183102 (2008).
[22]K. Ostrikov, I. Levchenko, and S. Xu, Pure Appl. Chem. **80**, 1909 (2008).
[23]H. Mehdipour and G. Foroutan, Phys. Plasmas **17**, 083704 (2010).
[24]I. Denysenko and K. Ostrikov, J. Phys. D: Appl. Phys. **42**, 015208 (2009).
[25]H. Mehdipour and K. Ostrikov, J. Am. Chem. Soc. **135**, 1912 (2013).
[26]G. Foroutan, H. Mehdipour, and H. Zahed, Phys. Plasmas **16**, 103703 (2009).
[27]B. P. Pandey, A. Samarian, and S. V. Vladimirov, Phys. Plasmas **14**, 093703 (2007).
[28]R. Chodura, Phys. Fluids **25**, 1628 (1982).
[29]H. Kersten, H. Deutsch, H. Steffen, G. M. W. Kroesen, and R. Hippler, Vaccum **63**, 385 (2001).
[30]F. Gibou, C. Ratsch, and R. Caflisch, Phys. Rev. B **67**, 155403 (2003).
[31]*CRC Handbook of Chemistry and Physics*, Internet Version, Sec. 12, 87th ed., edited by D. R. Lide (Taylor and Francis, Boca Raton, FL, 2007).
[32]J. D. Gale and J. M. Seddon, *Thermodynamics and Statistical Mechanics* (Wiley-Interscience, New York, 2002).
[33]C. Kittel, *Introduction to Solid State Physics*, 7th ed. (John Wiley & Sons, 1996).
[34]F. Rosei, J. Phys.: Condens. Matter **16**, S1373 (2004).
[35]Q. Cheng, S. Xu, J. Long, and K. Ostrikov, Appl. Phys. Lett. **90**, 173112 (2007).
[36]S. Y. Huang, Q. J. Cheng, S. Xu, D. Y. Wei, H. P. Zhou, J. D. Long, I. Levchenko, and K. Ostrikov, J. Appl. Phys. **111**, 036101 (2012).
[37]M. Lu, X. J. Yang, S. S. Perry, and J. W. Rabalais, Appl. Phys. Lett. **80**, 2096 (2002).
[38]K. Paredis, K. Vanormelingen, and A. Vantomme, Appl. Phys. Lett. **92**, 043111 (2008).